Mechanism of the strong magnetic refrigerant performance of $LaFe_{13-x}Si_x$

Michael D. Kuz'min and Manuel Richter
Leibniz-Institut für Festkörper-und Werkstoffforschung, IFW Dresden, PF 270116, D-01171 Dresden, Germany
(Received 21 June 2007; published 5 September 2007)

Electronic structure calculations reveal the presence of several shallow minima and maxima in the energy-vs-magnetization curves, which otherwise are surprisingly flat. The main implication—a fast magnetization and/or demagnetization process with little hysteresis—is of primary importance for the performance of $LaFe_{13-x}Si_x$ in magnetic cooling devices.

DOI: 10.1103/PhysRevB.76.092401 PACS number(s): 75.30.Sg, 71.20.Be, 75.50.Bb

The latest decade has witnessed a spectacular upsurge of interest in room-temperature magnetic refrigeration. The boom of research activity and the general expectation of an approaching technological breakthrough were brought about by the discovery of several materials with a so-called giant magnetocaloric effect.[1–3] Common to all these materials is that they undergo a first-order magnetic phase transition around room temperature. This gives rise to a sharp dependence of the magnetization on temperature near the transition point, which should also result in a large magnetic entropy change, if the Maxwell relation, $\partial S/\partial B = \partial M/\partial T$, were to be relied on. The latter cannot be taken for granted, however, because in the vicinity of a first-order phase transition a basic assumption of standard thermodynamics—that the system is continually at thermal equilibrium—usually fails. This failure manifests itself in slow dynamics and hysteresis, both of which hinder the use of the new materials in magnetic refrigerators, where high operation frequency and low hysteretic losses are essential.

$LaFe_{13-x}Si_x$ occupies a special place among the magnetic refrigerants of the new generation.[4,5] While enjoying in full measure the benefits of a first-order phase transition, $LaFe_{13-x}Si_x$ does not seem to have the disadvantages inherent therein. The most serious difficulty—hysteresis—is practically overcome in melt-spun $LaFe_{13-x}Si_x$ ribbons,[6] which offers the prospects of rapid magnetic cycling without loss of efficiency. Further strong points of $LaFe_{13-x}Si_x$ are the abundance of its main constituents, iron and silicon, and the possibility of adjusting the Curie point by varying x and/or by hydrogenation.[6,7]

A naturally arising question, what brings about this unusual combination of features characteristic of first- and second-order phase transitions that makes $LaFe_{13-x}Si_x$ so uniquely distinct, is addressed in this paper. As a method for our study we chose density-functional electronic structure calculations. These were carried out using the full-potential local-orbital program (FPLO,[8] version 5.00-19) in its scalar-relativistic mode. The exchange and correlation potential in the local spin-density approximation (LSDA) was taken in the form due to Perdew and Wang.[9] The valence basis states included 5*spd* and 6*sp* of La, 3*spd* and 4*sp* of Fe, as well as 3*spd* of Si. A reciprocal space mesh containing 72 k points within the irreducible wedge of the Brillouin zone was used to perform the self-consistent electronic structure calculations. For the one-step calculation of the density of states (DOS) the number of k points was increased to 2769.

$LaFe_{13-x}Si_x$ has the $NaZn_{13}$-type cubic structure (space group O_h^6-$Fm3c$) with eight formula units per conventional cell. The La atoms occupy the 8*a* sites $(\frac{1}{4}\frac{1}{4}\frac{1}{4})$, while Fe and Si are distributed at random between the 8*b* sites (000) and the 96*i* sites (0*yz*).[10] For simplicity we restricted ourselves to a special case of $x=1$ and further assumed that the 8*b* sites are occupied solely by silicon, while iron is located exclusively on the 96*i* sites. The internal positions of the latter were fixed at $y=0.179$ and $z=0.116$, as inferred from the powder neutron diffraction data.[10] For the lattice parameter a various values were taken, ranging from the experimental one, $a_{\text{exper}} \approx 11.5$ Å, down to the LSDA equilibrium value, $a_{\text{LSDA}} \approx 10.9$ Å (the latter is where the total energy computed in the LSDA is a minimum).

Our main effort was concentrated on so-called fixed-spin-moment (FSM) calculations, in which the numbers of valence electrons in both spin channels are fixed, rather than determined self-consistently as in the usual spin-polarized calculations. The FSM method, first proposed and implemented by Schwarz and Mohn over two decades ago,[11] is a standard technique for visualizing the presence of magnetically distinct states in a system.

Figure 1(a) displays four representative $E(M)$ curves calculated at the indicated values of the lattice parameter. Here M stands for the spin moment—the difference between the assumed electron occupation numbers in the majority and minority spin channels, while E is the computed total energy. The most salient feature of the curves in Fig. 1 is the presence of several shallow minima at certain stable abscissae, $M \approx 7$, 11, 21, and $25\mu_B$ per formula unit. According, as the lattice parameter increases from 11.1 Å to 11.4 Å, the global minimum in the $E(M)$ dependence migrates from ~7 to $25\mu_B$/f.u. This movement is essentially discontinuous: every time a new local minimum emerges in a set position, it coexists with the old one and eventually assumes the role of global minimum, while the former global minimum fades away.

Such FSM curves—with several shallow minima and maxima—-are characteristic of the entire iron-rich end of the $LaFe_{13-x}Si_x$ series, not just of the $x=1$ system. This point is illustrated in Fig. 1(b), where a similar dependence for the hypothetical end compound $LaFe_{13}$ is presented. This also suggests that the dubious preferential site occupation (assumed merely to avoid computationally tedious structural disorder) plays no major role here.

The reason why the curvature of the FSM profiles in Fig. 1 changes sign several times can be best explained with the

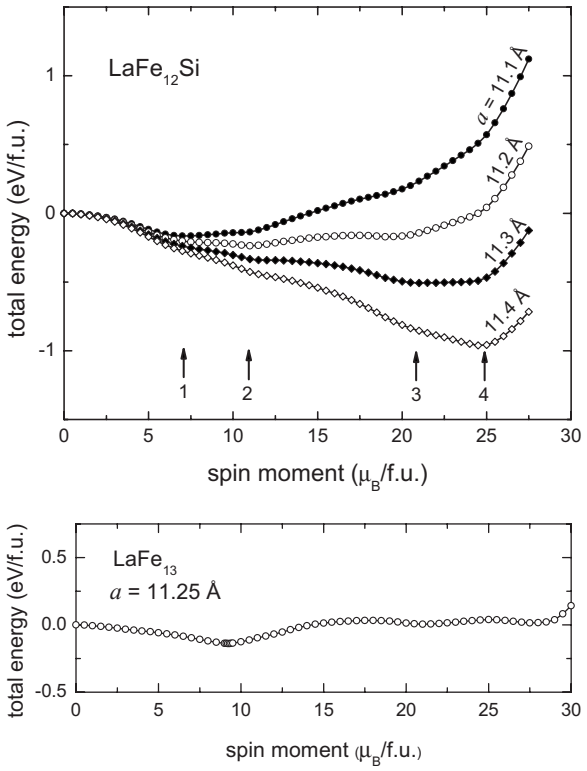

FIG. 1. Total energy vs spin magnetic moment, calculated at the indicated values of the lattice parameter.

help of the Stoner model of itinerant magnetism. In this model the reciprocal susceptibility, $\chi_M^{-1}=E''(M)$, is given by a simple formula[12]

$$\chi_M^{-1} = \mu_B^{-2}(D_M^{-1} - I), \tag{1}$$

where $I \sim 0.5$ eV is the Stoner parameter and D_M is the effective DOS at the Fermi level, defined by

$$D_M = \frac{4}{D_{M+}^{-1} + D_{M-}^{-1}}. \tag{2}$$

The Stoner theory adopts the rigid-band approximation, whereby the DOS of a spin-polarized state is obtained from the nonmagnetic DOS $D(E)$ by simply shifting the latter along the energy axis. Accordingly, the entering into Eq. (2) DOS at the Fermi level in the majority and minority subbands are given by $D_{M\pm}=\frac{1}{2}D(E_{F,M\pm})$, where the shifted Fermi levels are determined from an obvious condition,

$$\int_{E_{F,0}}^{E_{F,M\pm}} D(E)dE = \pm\frac{M}{2}, \tag{3}$$

$E_{F,0}$ being the Fermi energy of the unpolarized state. The somewhat heavy use of the subscript M in Eqs. (1)–(3) is to emphasize that the quantities defined therein are functions of the independent variable M, the spin magnetic moment.

Turning now to $LaFe_{12}Si$, its nonmagnetic DOS is presented in Fig. 2. The arrows mark the positions of the shifted Fermi level in the majority and/or minority subbands, the numbers corresponding to the labeling of the minima in

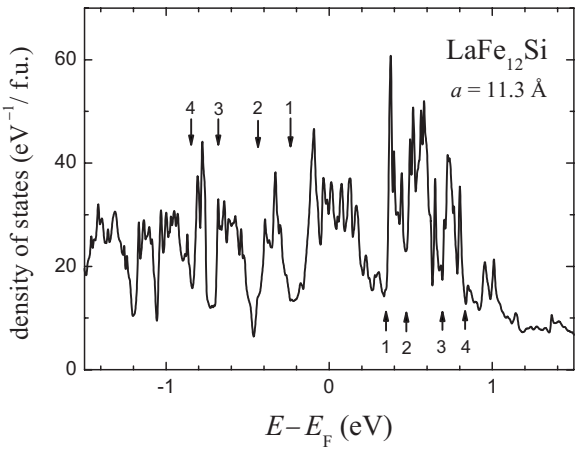

FIG. 2. Non-spin-polarized density of states of $LaFe_{12}Si$.

Fig. 1. In reality there is a finite interval of allowed M values around each arrow, wherein $\chi_M>0$ and $E(M)$ is curved upwards. The exact equilibrium positions within the intervals depend on the assumed value of the lattice parameter a. The allowed intervals are interlaid with forbidden ones, wherein the DOS at the Fermi level in *both* spin channels is so high that D_M exceeds I^{-1} and consequently χ_M is negative. Such forbidden values of M correspond to unstable states. The instability criterion, $ID_M>1$, is known as the generalized Stoner condition.[12]

Recapitulating, the Stoner theory links the oscillatory behavior of the FSM profiles of $LaFe_{12}Si$ (Fig. 1) to a series of high peaks and deep valleys in its DOS (Fig. 2). Earlier it was suggested[13] that the magnetic instability in $LaFe_{13-x}Si_x$ might be akin to that in face-centered-cubic (fcc) iron, where several magnetically distinct phases had been predicted.[14] This view was supported by an argument that the iron atoms situated on the 96*i* sites form icosahedral clusters similar to the coordination polyhedra in the fcc structure. Examining the DOS of fcc iron,[15] we found no narrow peaks or valleys that could enable us to draw a parallel between fcc Fe and $LaFe_{13-x}Si_x$. The preferred values of the atomic moments are also dissimilar: thus, the third minimum in Fig. 1(a) ($\sim 1.75\mu_B$/Fe atom) corresponds to a prominent maximum in the $E(M)$ dependence of fcc iron.[14] The two compounds are still broadly analogous, in the sense that the magnetic instability in both of them is governed by the generalized Stoner criterion, $ID_M>1$.

Our next goal is to find out what the FSM profile of an ideal magnetic refrigerant should look like. With this end in view, let us first clarify what determines the relative cooling power (RCP) of a refrigerant with a single first-order transition. An intersection point of the temperature dependences of the free energies of the two phases involved defines the transition temperature T_0, Fig. 3(a). The negative slopes of the two curves are the entropies $S_{1,2}$, the respective magnetizations being $M_{1,2}$. Assume for definiteness that $M_2>M_1$. Then a magnetic field B will suffice to induce a transition from phase 1 to phase 2 anywhere within the interval between T_0 and $T_0+\Delta T$, where ΔT is determined from an obvious condition, $\Delta T(S_1-S_2)=B(M_2-M_1)$. This will be accompanied by an entropy change of $\Delta S \equiv S_2-S_1$, see Fig.

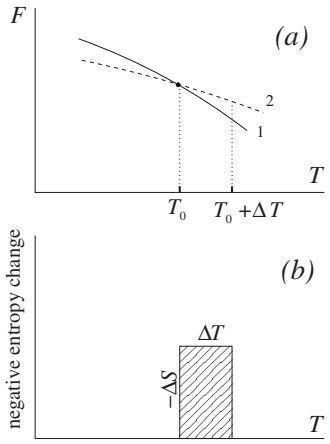

FIG. 3. Magnetic refrigerant undergoing a first-order phase transition: the free energies of the two phases in the absence of magnetic field (a), and the field-induced entropy change (b), plotted against temperature.

3(b). The hatched area under the curve equals the RCP as defined by Gschneidner and Pecharsky[16] (in real materials the peak is often trapezoid or caret shaped rather than rectangular). So we get

$$\mathrm{RCP} = B(M_2 - M_1). \tag{4}$$

Thus, for a given magnetic field the RCP of a refrigerant undergoing a first-order phase transition is determined solely by the difference of the magnetizations of the two phases.[17] Consequently, this key figure of merit is maximized by choosing materials whose FSM profiles have two minima situated as far apart as possible (Fig. 4).

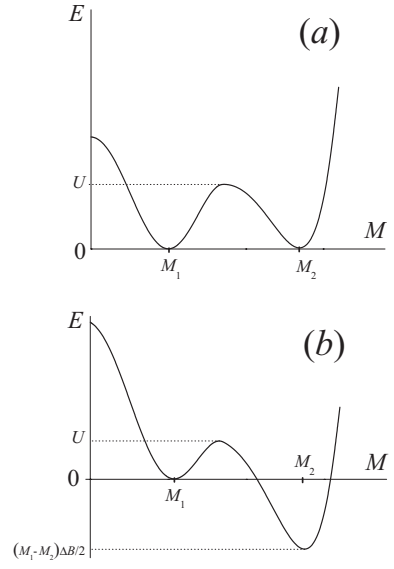

FIG. 4. Energy-vs-magnetization dependence of a hypothetical refrigerant undergoing a first-order phase transition. (a) The transition takes place quasistatically, the energies of the two phases are equal. (b) The transition $1 \rightarrow 2$ proceeds nonquasistatically in the presence of an extra magnetic field $\Delta B/2$ which favors the higher spin state and lowers the barrier.

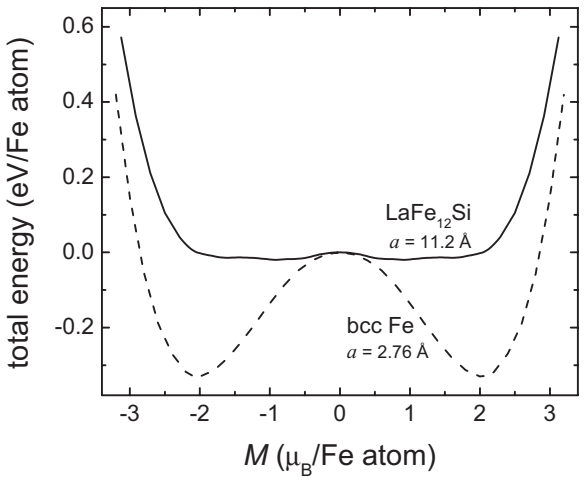

FIG. 5. Comparison of calculated $E(M)$ curves of $LaFe_{12}Si$ and bcc iron.

Equation (4) gives the *relative* (i.e., per refrigeration cycle) cooling power. The actual cooling power (measured in watts per unit volume) is a product of the RCP and the operation frequency f of the device. The upper bound for the latter quantity is normally set by the inertia of heat exchange at $\sim 2 \times 10^2$ Hz,[18] but it may be limited additionally by slow dynamics of the first-order phase transition. Overcoming the energy barrier between the two minima at $T \approx 300$ K is a thermally activated process, whose characteristic time constant is expected to obey the Arrhenius law

$$\tau = \tau_0 \exp\left(\frac{E_a}{kT}\right). \tag{5}$$

The prefactor in this formula is of the order of a femtosecond, $\tau_0 \sim \hbar/W \sim 10^{-15}$ s, where $W \sim 1$ eV is a characteristic bandwidth. For successful operation of a refrigerator it is necessary that $\tau f \ll 1$.[19]

When this condition is not fulfilled (i.e., in a nonquasistatic regime) the refrigerant may still undergo periodic first-order transitions accordingly as the magnetic field is cycled. However, there will be a difference (hysteresis) between the threshold fields of the transitions in the two directions. Consider, e.g., the transition $1 \rightarrow 2$ on rising the applied field. In quasistatic conditions it would occur at a certain critical field B_0, such that the energies of both phases are equal, as shown in Fig. 4(a). In a nonquasistatic regime, the transition takes place at a higher field, $B_0 + \Delta B/2$. The role of the extra field $\Delta B/2$ is to lower the barrier in the direction of the transition [i.e., from left to right in Fig. 4(b)] so that it can be overcome within the time small as compared with $1/f$. The energy difference between the final and the initial states, $(M_2 - M_1)\Delta B/2$, will be dissipated as heat. Similarly, the inverse transition $2 \rightarrow 1$ will take place at $B_0 - \Delta B/2$ on falling field and will be accompanied by dissipation of the same energy. The total amount of heat released in one cycle equals the area of the hysteresis loop, $(M_2 - M_1)\Delta B$. This amount should be deducted from the RCP, Eq. (4). Obviously, the broader the hysteresis, the less efficient is the operation of

the refrigerator. The cooling effect will be brought to nothing when the width of the hysteresis loop ΔB becomes as large as the maximum available field B. In reality, due to inevitable losses in the system, the cooling will cease at ΔB slightly less than B.

It is clear from the above discussion that the shape of the FSM profile plays an important role in the performance of magnetocaloric materials. Thus, a perfect refrigerant should have two minima far apart from each other separated by a possibly low barrier. Ideally, the profile between the minima should be flat, which is conceivable, if $D_M = \text{const} = I^{-1}$. As far as real solids are concerned, their DOS are generally known to be rapidly varying functions. Under the circumstances, the best behavior one could reasonably expect of the effective DOS is that for $M_1 < M < M_2$, D_M oscillates possibly close to I^{-1}, so that the curvature of the FSM profile χ_M^{-1} oscillates about zero.

$LaFe_{12}Si$ does seem to fit this description. From comparison with body-centered-cubic (bcc) iron, Fig. 5, one can appreciate that $LaFe_{12}Si$ has indeed a flat-bottomed FSM profile. Perhaps, as flat-bottomed as one may hope to find in a solid.

Summarizing, our density-functional calculations demonstrate that the first-order magnetic transition in $LaFe_{13-x}Si_x$ is in fact a series of three consecutive first-order transitions. The reason is that the energy-vs-magnetization dependence of $LaFe_{13-x}Si_x$ has an extensive flat bottom part, with several shallow minima and maxima. This fact is of substantial benefit to the magnetocaloric properties of this promising material, because lower energy barriers between the various spin states mean faster magnetization and/or demagnetization with less hysteresis.

This work was financially supported by Deutsche Forschungsgemeinschaft Contract No. RI 932/4-1.

[1] V. K. Pecharsky and K. A. Gschneidner, Jr., Phys. Rev. Lett. **78**, 4494 (1997).
[2] X. X. Zhang, G. H. Wen, F. W. Wang, W. H. Wang, C. H. Yu, and G. H. Wu, Appl. Phys. Lett. **77**, 3072 (2000).
[3] O. Tegus, E. Brück, K. H. J. Buschow, and F. R. de Boer, Nature (London) **415**, 150 (2002).
[4] A. Fujita, K. Fukamichi, J.-T. Wang, and Y. Kawazoe, Phys. Rev. B **68**, 104431 (2003).
[5] A. Fujita, K. Fukamichi, M. Yamada, and T. Goto, Phys. Rev. B **73**, 104420 (2006).
[6] O. Gutfleisch, A. Yan, and K.-H. Müller, J. Appl. Phys. **97**, 10M305 (2005).
[7] K. Mandal, O. Gutfleisch, A. Yan, A. Handstein, and K.-H. Müller, J. Magn. Magn. Mater. **290-291**, 673 (2005).
[8] K. Koepernik and H. Eschrig, Phys. Rev. B **59**, 1743 (1999); http://www.FPLO.de
[9] J. P. Perdew and Y. Wang, Phys. Rev. B **45**, 13244 (1992).
[10] F. Wang, G. Wang, F. Hu, A. Kurbakov, B. Shen, and Z. Cheng, J. Phys.: Condens. Matter **15**, 5269 (2003).
[11] K. Schwarz and P. Mohn, J. Phys. F: Met. Phys. **14**, L129 (1984).
[12] J. Kübler, *Theory of Itinerant Electron Magnetism* (Clarendon, Oxford, 2000), Chap. 4.
[13] A. Fujita, Y. Akamatsu, and K. Fukamichi, J. Appl. Phys. **85**, 4756 (1999).
[14] P. M. Marcus, S. L. Qiu, and V. L. Moruzzi, J. Phys.: Condens. Matter **11**, 5709 (1999).
[15] J. Kübler, Phys. Lett. **81A**, 81 (1981).
[16] K. A. Gschneidner, Jr. and V. K. Pecharsky, Annu. Rev. Mater. Sci. **30**, 387 (2000).
[17] A. Fujita, S. Fujieda, and K. Fukamichi, J. Magn. Magn. Mater. **310**, e1006 (2007).
[18] M. D. Kuz'min, Appl. Phys. Lett. **90**, 251916 (2007).
[19] It should be noted that the activation energy E_a in the Arrhenius formula (5) cannot be simply identified with the height of the energy barrier U obtained in electronic structure calculations, Fig. 4. The latter has the dimensionality of energy per unit volume (or per formula unit, etc.). Direct proportionality between the two quantities is to be expected, however, the coefficient of proportionality (activation volume or similar) is essentially unknown.